DOI: 10.1002/ejic.200700113

Coordinated 1,3-Diyne Diols as Organometallic Building Blocks for Large Macrocycles Containing Oxygen and Unsaturated Donor Units

Louisa J. Hope-Weeks,*[a] Martin J. Mays,[b] and Gregory A. Solan*[c]

Keywords: Macrocycles / Cobalt complexes / Oxygen / Alkynes / Nicholas reaction

The acid-catalysed reaction of $[\{Co_2(CO)_6(\mu\text{-}\eta^2\text{-}HOCH_2C_2\text{-})\}_2]$ (**1a**) with a range of alkyl diols has been examined as means of preparing large crown-type macrocycles (up to twenty eight-membered) containing at least one coordinated 1,3-diyne unit, multiple oxygen atoms and a variety of soft donor units. Thus, interaction of **1a** with $HOCH_2(CH_2)_nCH_2OH$, allows access to the monomeric cyclised complexes $[\{Co_2(CO)_6\}_2\{cyclo\text{-}\mu\text{-}\eta^2\text{:}\mu\text{-}\eta^2\text{-}CH_2C_2C_2CH_2OCH_2(CH_2)_nCH_2O\}]$ (**3a**: $n = 2$, **3b**: $n = 3$, **3c**: $n = 4$) along with the dimeric cyclised species $[\{Co_2(CO)_6\}_2\{cyclo\text{-}\mu\text{-}\eta^2\text{:}\mu\text{-}\eta^2\text{-}CH_2C_2C_2CH_2OCH_2(CH_2)_nCH_2O\}]_2$ (**4a**: $n = 2$, **4b**: $n = 3$, **4c**: $n = 4$). Introduction of additional oxygen donor atoms into the macrocycle can be achieved by reaction of **1a** with the glycols, $HO(CH_2CH_2O)_nH$, to afford exclusively monomeric $[\{Co_2(CO)_6\}_2\{cyclo\text{-}\mu\text{-}\eta^2\text{:}\mu\text{-}\eta^2\text{-}CH_2C_2C_2CH_2O(CH_2CH_2O)_n\}]$ (**5a**: $n = 3$, **5b**: $n = 4$). On the other hand, treatment of **1a** with the 1,3-diyne-linked alkyl diols, $HOCR_2C{\equiv}CC{\equiv}CCR_2OH$, furnishes the more rigid monomeric $[\{Co_2(CO)_6\}_2\{cyclo\text{-}\mu\text{-}\eta^2\text{:}\mu\text{-}\eta^2\text{-}CH_2C_2C_2CH_2OCR_2C_2C_2CR_2O\}]$ [**6a**: R = H, **6b**: R = Me] and dimeric macrocycles $[\{Co_2(CO)_6\}_2\{cyclo\text{-}\mu\text{-}\eta^2\text{:}\mu\text{-}\eta^2\text{-}CH_2C_2C_2CH_2OCR_2C_2C_2CR_2O\}]_2$ [**7a**: R = H, **7b**: R = Me], whereas the use of the alkynyl- or aryl-linked alkyl diols, $HOCH_2(L)CH_2OH$, affords the unsymmetrical dimeric $[\{Co_2(CO)_6\}_2\{cyclo\text{-}\mu\text{-}\eta^2\text{:}\mu\text{-}\eta^2\text{-}CH_2C_2C_2CH_2\}_2O\{OCH_2(L)CH_2O\}]$ [**8a**: L = $-C{\equiv}C-$, **8b**: L = 1,4-C_6H_4] and symmetrical dimeric species $[\{Co_2(CO)_6\}_2\{cyclo\text{-}\mu\text{-}\eta^2\text{:}\mu\text{-}\eta^2\text{-}CH_2C_2C_2CH_2OCH_2(L)CH_2O\}]_2$ [**9a**: L = $-C{\equiv}C-$, **9b**: L = 1,4-C_6H_4]. Also isolated as a by-product from all the above reactions is the self-dimerised macrocycle $[\{Co_2(CO)_6\}_2\{cyclo\text{-}\mu\text{-}\eta^2\text{:}\mu\text{-}\eta^2\text{-}CH_2C_2C_2CH_2O\}]_2$ (**2**) which can itself be synthesised more directly by treating **1a** with catalytic quantities of $HBF_4{\cdot}OEt_2$. Single crystal X-ray diffraction studies have been performed on **2**, **3a**, **5a**, **7a**, **8a**, **8b** and **9a**.

Introduction

Recent years have seen a surge of interest in the application of the acid-catalysed Nicholas reaction (both intra- and intermolecular)[1] to promote the formation of both carbocyclic and heteroatom-containing medium to large ring systems.[1d,2–6,9–11] This can, in part, be attributed to the connection the resultant materials have to either natural products,[2,4] bio-inorganic hosts,[7] molecular sensors[7] or to nanomaterials.[8] With regard to intermolecular reactions, the reactivity of hexacarbonyldicobalt-coordinated monoyne diols, $[\{Co_2(CO)_6(\mu\text{-}\eta^2\text{-}HOCR_2C{\equiv}CR_2OH)\}]$ (R = H, hydrocarbyl), towards a range of nucleophiles has been extensively investigated by Went and co-workers and allows access to a rich variety of medium to large macrocycles containing an assortment of donor functionalities.[3] On the other hand, the use of the more extended bis(hexacarbonyldicobalt)-coordinated diyne diols (and ethers) has received less attention with a few reports focusing on the reactivity of organo-linked diyne derivatives.[4–6] In our programme, we have found that the less flexible and conjugated 1,3-diyne diol, $[\{Co_2(CO)_6(\mu\text{-}\eta^2\text{-}HOCH_2C_2\text{-})\}_2]$ (**1a**, Figure 1), can also serve as a pre-organised building block for the assembly of ring systems including large thio- and mixed S,O-macrocycles.[9,10] Significantly, the use of the more bulky $[\{Co_2(CO)_6(\mu\text{-}\eta^2\text{-}HOCMe_2C_2\text{-})\}_2]$ (**1b**) inhibits an intermolecular reaction and instead generates a strained seven-membered ring carbocycle via an intramolecular pathway.[11]

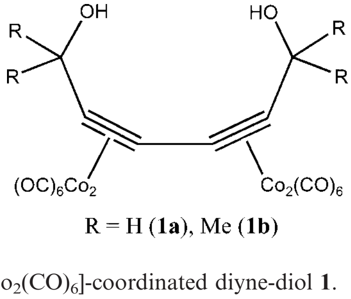

R = H (**1a**), Me (**1b**)

Figure 1. Bis[$Co_2(CO)_6$]-coordinated diyne-diol **1**.

As an extension to our work in this area, we have been interested in employing the Nicholas reaction to generate crown-type macrocycles that can additionally incorporate soft donor groups such as 1,3-diynes, alkynes and aryls groups. To this end we have targeted a family of alkyl diols,

---

[a] Department of Chemistry and Biochemistry, Texas Tech University,
Lubbock, TX 79409-1061, USA
[b] Department of Chemistry,
Lensfield Road, Cambridge CB2 1EW, UK
[c] Department of Chemistry, University of Leicester,
University Road, Leicester LE1 7RH, UK
E-mail: gas8@leicester.ac.uk

$HOCR_2$-linker-CR_2OH (linker = alkyl, glycol, 1,3-diynyl, alkynyl, aryl; R = H, Me), as potential nucleophiles for the acid-catalysed reaction with the less sterically encumbered **1a**. Herein, we report full details of our findings from this study.

Results and Discussion

1. Reactions of 1a with Alkyl Diols

The reaction of $[\{Co_2(CO)_6(\mu\text{-}\eta^2\text{-}HOCH_2C_2\text{-})\}_2]$ (**1a**) with one equivalent of $HOCH_2(CH_2)_nCH_2OH$ (n = 2–4) in dichloromethane at –78 °C in the presence of $HBF_4{\cdot}OEt_2$ gave the self-dimerised product $[\{Co_2(CO)_6\}_2\{\mathit{cyclo}\text{-}\mu\text{-}\eta^2\text{:}\mu\text{-}\eta^2\text{-}CH_2C_2C_2CH_2O\}]_2$ (**2**), the monomeric cyclised complexes $[\{Co_2(CO)_6\}_2\{\mathit{cyclo}\text{-}\mu\text{-}\eta^2\text{:}\mu\text{-}\eta^2\text{-}CH_2C_2C_2CH_2OCH_2(CH_2)_nCH_2O\}]$ (**3a**: n = 2, **3b**: n = 3, **3c**: n = 4) and the dimeric cyclised species $[\{Co_2(CO)_6\}_2\{\mathit{cyclo}\text{-}\mu\text{-}\eta^2\text{:}\mu\text{-}\eta^2\text{-}CH_2C_2C_2CH_2OCH_2(CH_2)_nCH_2O\}]_2$ (**4a**: n = 2, **4b**: n = 3, **4c**: n = 4) in high combined yield (Scheme 1). Complex **2** can also be obtained by stirring **1a** in dichloromethane in the presence of $HBF_4{\cdot}OEt_2$. The complexes **2**–**4** have been characterised by FAB mass spectrometry and by ^1H and ^{13}C NMR and IR spectroscopy (see Table 1 and experimental section). Satisfactory microanalytical data were obtained for all complexes. In addition, the complexes **2** and **3a** have been the subject of single-crystal X-ray diffraction studies.

Suitable crystals of **2** and **3a** for the X-ray determination were grown from dichloromethane by slow diffusion of hexane at 0 °C. Perspective views of **2** and **3a** are depicted in Figures 2 and 3; selected bond lengths and angles are listed in Tables 2 and 3. The molecular structure of **2** contains a crystallographic centre of symmetry which lies at the midpoint of the C(18)–C(13A) and C(13)–C(18A) alkynic bonds. The structure itself is based on a fourteen-membered 1,8-dioxacyclotetradeca-3,5,10,12-tetrayne ring with the two diyne units each coordinated by two $Co_2(CO)_6$ units in an η^2:η^2 fashion. The Co_2C_2 cores adopt the expected tetrahedral arrangements with the bond parameters falling within the normal range.[12–14] Within each coordinated diyne unit the two Co_2C_2 units are disposed in a pseudo *cis* configuration [torsion angle C(16)–C(17)–C(18)–C(13A) 36.5°] with the C≡C–CH_2 *bend-back* angles[15] [C(15)–C(16)–C(17) 141.5(2), C(18A)–C(13)–C(14) 144.5(2)°] similar to those observed in related acyclic cobalt–alkyne complexes;[12,13] the mean C≡C–CH_2 angle is 141.31°.[16]

Complex **3a** crystallises with two discrete independent molecules (A and B in Table 3) within its asymmetric unit. The main difference between the two molecules is the presence of some disorder within the O(16)–C(17)–C(18)–C(19)

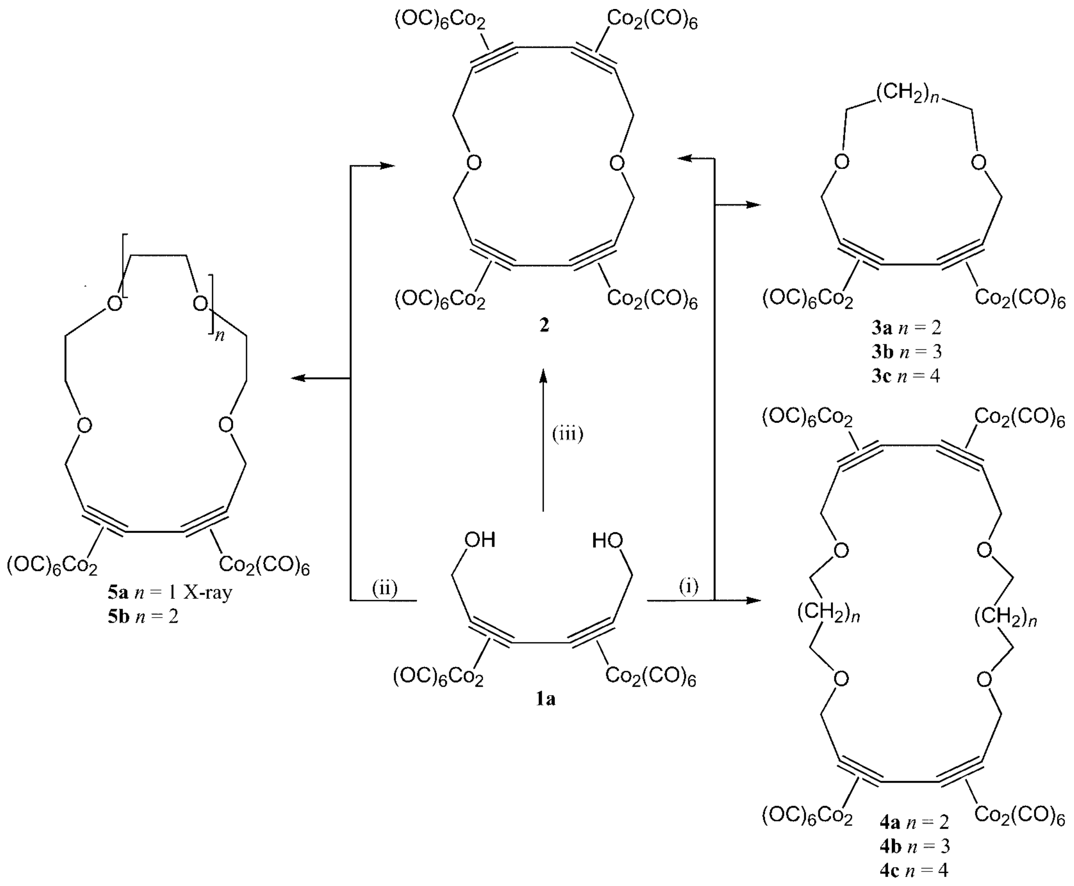

Scheme 1. Reagents and conditions; (i) $HOCH_2(CH_2)_nCH_2OH$, $HBF_4{\cdot}OEt_2$ (cat.), –78 °C, CH_2Cl_2; (ii) $HO(CH_2CH_2O)_nH$, $HBF_4{\cdot}OEt_2$ (cat.), –78 °C, CH_2Cl_2; (iii) $HBF_4{\cdot}OEt_2$ (cat.), –78 °C, CH_2Cl_2.

Table 1. Spectroscopic and analytical data for the new complexes **2**–**9**.

	ν(CO) [cm^{-1}][a]	^{1}H NMR [δ][b]	FAB mass spectrum	Microanalysis [%][c]	
				C	H
2	2025 (s), 2062 (s), 2083 (s), 2100 (m)	4.93 (s, 8 H, CCH_2O)	M$^+$ (1328), M$^+$ – *n*CO (*n* = 1–24)	32.65 (32.56)	0.71 (0.61)
3a	2027 (s), 2063 (vs), 2083 (s), 2101 (m)	4.67 (s, 4 H, CCH_2O), 3.57 [br. s, 4 H, $OC\mathit{H}_2(CH_2)_2C\mathit{H}_2O$], 1.67 [br. s, 4 H, $OCH_2(C\mathit{H}_2)_2CH_2O$]	M$^+$ (736), M$^+$ – *n*CO (*n* = 1–12)	36.02 (35.90)	1.66 (1.64)
3b	2024 (s), 2059 (vs), 2082 (s), 2100 (m)	4.68 (s, 4 H, CCH_2O), 3.48 [br. s, 4 H, $OC\mathit{H}_2(CH_2)_3C\mathit{H}_2O$], 1.5–1.3 [m, 6 H, $OCH_2(C\mathit{H}_2)_3CH_2O$]	M$^+$ (750), M$^+$ – *n*CO (*n* = 1–12)	37.01 (36.81)	1.91 (1.87)
3c	2023 (s), 2058 (vs), 2082 (s), 2102 (m)	4.57 (s, 4 H, CCH_2O), 3.57 [m, 4 H, $OC\mathit{H}_2(CH_2)_4C\mathit{H}_2O$], 1.5–1.3 [m, 8 H, $OCH_2(C\mathit{H}_2)_4CH_2O$]	M$^+$ (764), M$^+$ – *n*CO (*n* = 1–12)	37.24 (37.73)	2.14 (2.11)
4a	2024 (s), 2059 (vs), 2081 (s), 2101 (m)	4.66 (s, 8 H, CCH_2O), 3.73 [br. s, 8 H, $OC\mathit{H}_2(CH_2)_2C\mathit{H}_2O$], 1.70 [br. s, 8 H, $OCH_2(C\mathit{H}_2)_2CH_2O$]	M$^+$ (1472), M$^+$ – *n*CO (*n* = 1–24)	36.08 (35.90)	1.76 (1.64)
4b	2025 (s), 2059 (vs), 2082 (m), 2101 (m)	4.67 (s, 8 H, CCH_2O), 3.60 [m, 8 H, $OC\mathit{H}_2(CH_2)_3C\mathit{H}_2O$], 1.6–1.4 [m, 12 H, $OCH_2(C\mathit{H}_2)_3CH_2O$]	M$^+$ (1500), M$^+$ – *n*CO (*n* = 1–24)	37.05 (36.81)	2.01 (1.87)
4c	2025 (s), 2058 (vs), 2082 (s), 2101 (m)	4.59 (s, 8 H, CCH_2O), 3.51 [m, 8 H, $OC\mathit{H}_2CH_2(CH_2)_2CH_2C\mathit{H}_2O$], 1.55 [br. s, 8 H, $CH_2C\mathit{H}_2(CH_2)_2C\mathit{H}_2CH_2O$], 1.29 [br. s, 8 H, $CH_2CH_2(C\mathit{H}_2)_2CH_2CH_2O$]	M$^+$ (1528), M$^+$ – *n*CO (*n* = 1–24)	36.92 (37.73)	2.05 (2.11)
5a	2026 (s), 2062 (vs), 2084 (s), 2102 (m)	4.82 (s, 4 H, CCH_2O), 3.8–3.5 [m, 12 H, $O(CH_2CH_2O)_3$]	M$^+$ (796), M$^+$ – *n*CO (*n* = 1–12)	36.22 (36.21)	1.96 (2.03)
5b	2025 (s), 2059 (vs), 2082 (s), 2101 (m)	4.77 (s, 4 H, CCH_2O), 3.8–3.6 [m, 16 H, $O(CH_2CH_2O)_4$]	M$^+$ (840), M$^+$ – *n*CO (*n* = 1–12)	37.34 (37.17)	2.22 (2.40)
6a	2027 (s), 2059 (vs), 2084 (s), 2102 (m)	4.95 (s, 4 H, CCH_2O), 4.33 (s, 4 H, CCH_2O)	M$^+$ (756), M$^+$ – *n*CO (*n* = 1–12)	38.41 (38.13)	1.31 (1.07)
6b	2030 (s), 2057 (vs), 2084 (s), 2093 (w), 2102 (w)	4.96 (s, 4 H, CCH_2O), 1.41 (s, 12 H, CH_3)	M$^+$ (812), M$^+$ – *n*CO (*n* = 1–12)	–	–
7a	2027 (s), 2058 (vs), 2084 (s), 2103 (m)	4.74 (s, 8 H, CCH_2O), 4.42 (s, 8 H, CCH_2O)	M$^+$ (1512), M$^+$ – *n*CO (*n* = 1–24)	38.48 (38.13)	1.01 (1.07)
7b	2030 (s), 2061 (vs), 2083 (s), 2102 (w)	4.12 (s, 8 H, CCH_2O), 1.23 (s, 24 H, CH_3)	M$^+$ (1624), M$^+$ – *n*CO (*n* = 1–24)	40.76 (39.93)	1.42 (1.29)
8a	2015 (sh), 2031 (m), 2056 (m), 2065 (vs), 2085 (m), 2102 (m)	5.10 (s, 4 H, CCH_2O), 4.79 (s, 4 H, CCH_2O), 4.39 (s, 4 H, CCH_2O)	M$^+$ (1396), M$^+$ – *n*CO (*n* = 1–24)	35.66 (35.89)[d]	1.45 (1.33)[d]
8b	2024 (s), 2035 (m), 2058 (s), 2064 (vs), 2083 (s), 2101 (m)	7.37 (br. s, 4 H, Ph), 4.86 (s, 4 H, CCH_2O), 4.54 (s, 4 H, CCH_2O), 4.09 (s, 4 H, CCH_2O)	M$^+$ (1448), M$^+$ – *n*CO (*n* = 1 – 24)	36.12 (36.50)	1.22 (1.11)
9a	2029 (s), 2061 (s), 2085 (s), 2103 (m)	4.74 (s, 8 H, CCH_2O), 4.42 (s, 8 H, CCH_2O)	M$^+$ (1464), M$^+$ – *n*CO (*n* = 1–24)	36.07 (36.10)	1.22 (1.10)
9b	2027 (s), 2059 (vs), 2083 (s), 2102 (w)	7.5–7.3 (m, 8 H, Ph), 4.50 (s, 8 H, CCH_2O), 4.48 (s, 8 H, CCH_2O)	M$^+$ (1568), M$^+$ – *n*CO (*n* = 1–24)	39.79 (39.83)	1.68 (1.54)

[a] CH_2Cl_2 solution, 0.5 mm NaCl cells. [b] ^{1}H NMR chemical shifts in ppm relative to $SiMe_4$ (δ = 0.0 ppm), coupling constants in Hz in $CDCl_3$ at 293 K. [c] Calculated values shown in parentheses. [d] Calculated values include 0.5 hexane.

section of the ring in molecule A which is absent in B. The molecular structure consists of a twelve-membered 1,6-dioxacyclododeca-8,10-diyne macrocyclic ring with the diyne section coordinated by two $Co_2(CO)_6$ units and linked at each end by a $CH_2OCH_2CH_2CH_2CH_2OCH_2$ chain. The Co_2C_2 cores adopt the expected tetrahedral arrangements with the metal–metal bonds of each being located almost perpendicular to the corresponding alkyne vectors and their lengths falling in the expected ranges.[12–14] Inspection of the C≡C–C≡C torsion angle within the coordinated 1,3-diyne section of the macrocycle also reveals some differences between the independent molecules [torsion angle C(14)–C(13)–C(24)–C(23) 50.7° (molecule A), 44.2° (molecule B)] with the mean value ca. 11° larger than that in **2**. The *bend back* angles within and between molecules are similar [140.7(3), 140.2(3) (molecule A) vs. 138.6(3), 140.4(4)° (molecule B)] and as with **2** comparable with those found in related non-cyclic 1,3-diyne cobalt carbonyl complexes.[12,13]

The IR spectra of **2**–**4** reveal terminal carbonyl bands with patterns similar to that for **1a**[17] and to other bis(hexacarbonyldicobalt)-protected 1,3-diyne complexes.[13] In their FAB mass spectra, molecular ions are clearly visible along with fragmentation peaks corresponding to the loss of carbonyl groups from the corresponding molecular ion. In the ^{1}H NMR spectra of **2**–**4**, the protons for the methylene groups adjacent to both an alkynic carbon atom and an oxygen atom are seen as singlets in the range δ = 4.57–4.93 while the aliphatic chain CH_2 groups in **3** and **4** are seen more upfield. Due to the high degree of symmetry as

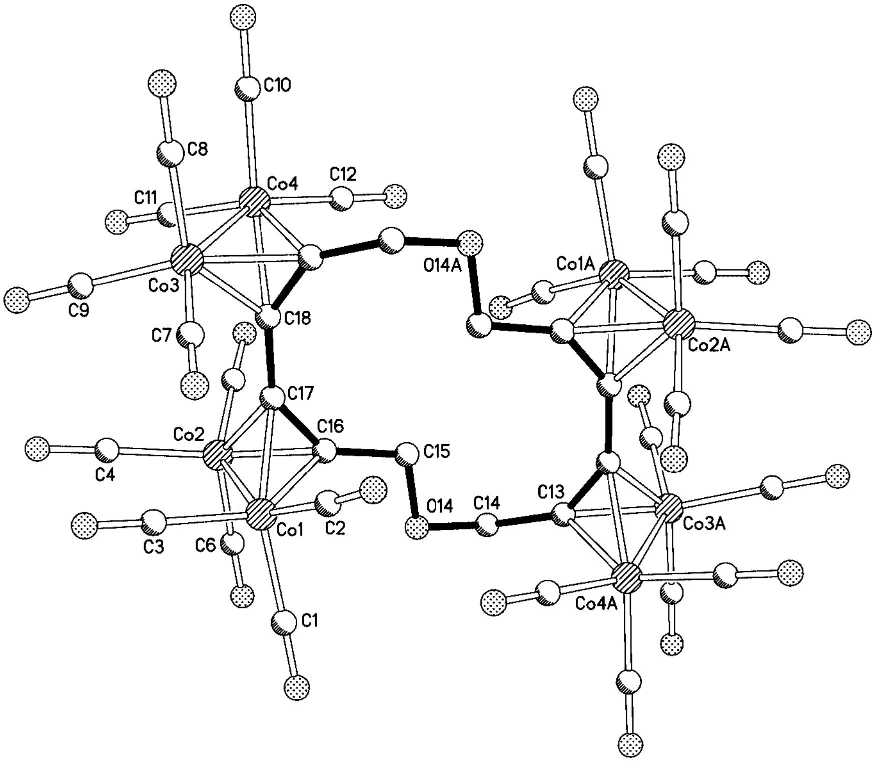

Figure 2. Molecular structure of **2** with partial atom labeling Scheme; all hydrogen atoms have been omitted for clarity.

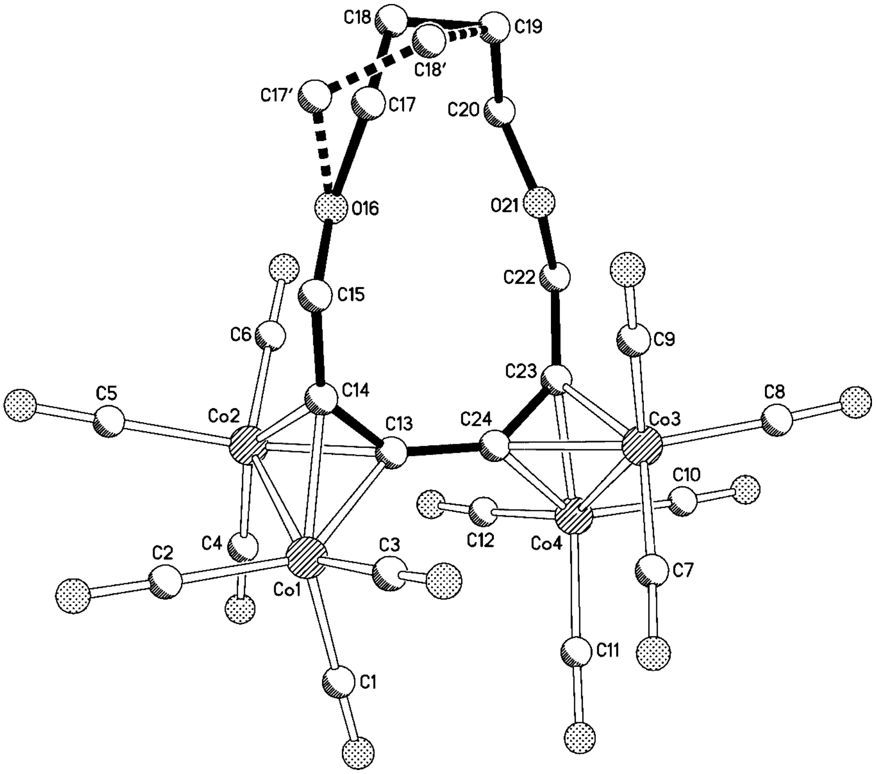

Figure 3. Molecular structure of **3a** with partial atom labeling scheme; all hydrogen atoms have been omitted for clarity (the dotted line indicates the disordered moiety).

Table 2. Selected bond lengths [Å] and angles (°) for **2**.[a]

Bond lengths			
C(13)–C(14)	1.497(3)	C(18)–C(13A)	1.362(3)
C(14)–O(14)	1.426(2)	Co(1)–Co(2)	2.4700(3)
C(15)–O(14)	1.419(2)	Co(3)–Co(4)	2.4626(4)
C(15)–C(16)	1.479(3)	Co–C(carbonyl)	1.787(2)–1.831(2)
C(16)–C(17)	1.363(3)	C–O(carbonyl)	1.125(3)–1.140(2)
C(17)–C(18)	1.432(3)	Co–C(alkyne)	1.941(2)–1.980(2)
Bond angles			
C(18A)–C(13)–C(14)	144.5(2)	C(15)–C(16)–C(17)	141.5(2)
C(13)–C(14)–O(14)	115.29(15)	C(16)–C(17)–C(18)	143.5(2)
C(14)–O(14)–C(15)	110.86(14)	C(17)–C(18)–C(13A)	145.4(2)
O(14)–C(15)–C(16)	110.9(2)		

[a] Atoms with suffix A are generated by symmetry (–*x*, 1 – *y*, –*z*).

Table 3. Selected bond lengths [Å] and angles (°) for **3a**.

	Molecule A	Molecule B
Bond lengths		
C(13)–C(14)	1.353(4)	1.350(4)
C(14)–C(15)	1.482(4)	1.484(4)
C(15)–O(16)	1.406(4)	1.427(3)
O(16)–C(17)	1.521(7)	1.433(4)
C(17)–C(18)	1.549(8)	1.499(5)
C(18)–C(19)	1.408(6)	1.535(5)
C(19)–C(20)	1.486(5)	1.489(5)
C(20)–O(21)	1.370(4)	1.414(4)
O(21)–C(22)	1.431(4)	1.415(4)
C(22)–C(23)	1.477(4)	1.479(4)
C(23)–C(24)	1.353(4)	1.352(4)
C(24)–C(13)	1.420(4)	1.426(4)
Co(1)–Co(2)	2.4588(5)	2.4646(5)
Co(3)–Co(4)	2.4717(5)	2.4692(5)
Co–C(carbonyl)	1.787(2)–1.831(2)	1.787(2)–1.831(2)
C–O(carbonyl)	1.125(3)–1.140(2)	1.125(3)–1.140(2)
Co–C(alkyne)	1.941(2)–1.980(2)	1.941(2)–1.980(2)
Bond angles		
C(13)–C(14)–C(15)	140.2(3)	140.4(3)
C(14)–C(15)–O(16)	107.6(2)	108.1(2)
C(15)–O(16)–C(17)	107.9(3)	112.9(2)
O(16)–C(17)–C(18)	104.3(5)	113.3(3)
C(17)–C(18)–C(19)	116.1(5)	115.2(3)
C(18)–C(19)–C(20)	113.6(4)	116.1(3)
C(19)–C(20)–O(21)	109.2(3)	110.1(3)
C(20)–O(21)–C(22)	113.1(3)	112.4(4)
O(21)–C(22)–C(23)	106.7(3)	108.9(2)
C(22)–C(23)–C(24)	140.7(3)	138.6(3)
C(23)–C(24)–C(13)	141.5(3)	141.2(3)

well as the quadrupole broadening due to ^{59}Co, the NMR spectroscopic data for monomeric **3** and its respective dimer **4** are virtually indistinguishable.

2. Reaction of 1a with Glycols

With the intent of introducing additional hard oxygen donor functionality into the macrocycle, the reaction of **1a** with two types of glycol was examined. Thus, treatment of **1a** with one equivalent of $HO(CH_2CH_2O)_nH$ ($n = 3, 4$) in dichloromethane at –78 °C in the presence of $HBF_4{\cdot}OEt_2$ gave the monomeric cyclised complexes [{$Co_2(CO)_6$}$_2$-{*cyclo*-μ-η^2:μ-η^2-$CH_2C_2C_2CH_2O(CH_2CH_2O)_n$}] (**5a**: $n = 3$, **5b**: $n = 4$) in high yield (Scheme 1). As with the reactions of **1a** with $HO(CH_2)_nOH$ (vide supra), **2** was isolated as a minor by-product in each case. Both new complexes have been characterised by mass spectrometry and by ^{1}H, ^{13}C NMR and IR spectroscopy (see Table 1 and Experimental section). Satisfactory microanalytical data were obtained for both **5a** and **5b**. In addition, **5a** has been the subject of a single-crystal X-ray diffraction study.

Single crystals of **5a** suitable for the X-ray determination were grown from hexane by slow evaporation at 0 °C. A view of the structure is depicted in Figure 4; selected bond lengths and angles are given in Table 4. The structure consists of a sixteen-membered 1,4,7,10-tetraoxacyclohexadeca-12,14-diyne ring with the two methylene end groups of the coordinated $CH_2C{\equiv}C{-}C{\equiv}CCH_2$ moiety linked by a triethyleneglycol-derived tether. Within the Co_2C_2 tetrahedral cores there are no unusual structural features, with all bond lengths and angles falling in the expected ranges.[12–14] The relative disposition of the two Co_2C_2 fragments can be described as pseudo *cis* [torsion angle C(14)–C(15)–C(16)–C(17) 45.6°] while the two $CH_2{-}C{\equiv}C$ *bend back* angles are comparable [C(13)–C(14)–C(15) 142.05(19) vs. C(16)–C(17)–C(18) 140.9(2)°]. An approximation of the cavity size can be made by studying the non-bonding oxygen–oxygen separations [O(13)···O(14) 2.916, O(13)···O(15) 4.730, O(13)···O(16) 5.240, O(14)···O(16) 4.800 Å] which can be compared to the non-bonding O–O separations of 4.362, 3.012 and 2.971 Å in 12-crown-4.[18]

The ^{1}H NMR spectra of **5a** and **5b** are similar with the methylene protons on the OCH_2 groups adjacent to the alkynic carbons taking the form of a singlet at ca. 4.80 while the OCH_2CH_2O protons are seen as multiplets in the range $\delta = 3.82–3.56$. The ^{13}C NMR spectra are also similar but differ with two resonances seen for the methylene carbons

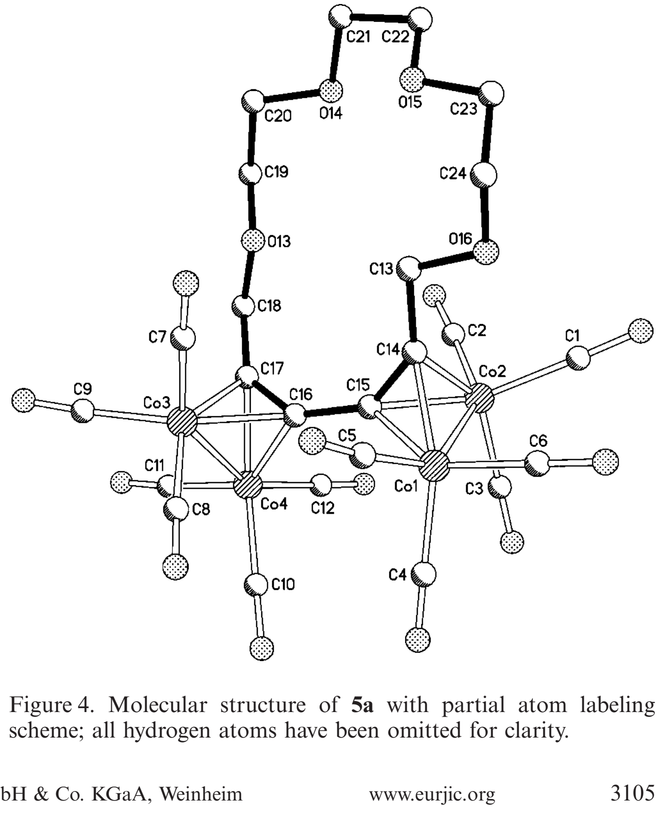

Figure 4. Molecular structure of **5a** with partial atom labeling scheme; all hydrogen atoms have been omitted for clarity.

Table 4. Selected bond lengths [Å] and angles (°) for **5a**.

Bond lengths			
C(13)–C(14)	1.480(3)	C(22)–O(15)	1.413(3)
C(14)–C(15)	1.358(3)	O(15)–C(23)	1.415(3)
C(15)–C(16)	1.429(3)	C(23)–C(24)	1.493(3)
C(16)–C(17)	1.352(3)	C(24)–O(16)	1.430(2)
C(17)–C(18)	1.485(3)	O(16)–C(13)	1.421(2)
C(18)–O(13)	1.410(3)	Co(1)–Co(2)	2.4710(4)
O(13)–C(19)	1.424(3)	Co(3)–Co(4)	2.4715(4)
C(19)–C(20)	1.494(3)	Co–C(carbonyl)	1.784(3)–1.828(3)
C(20)–O(14)	1.412(3)	C–O(carbonyl)	1.129(3)–1.141(3)
O(14)–C(21)	1.426(3)	Co–C(alkyne)	1.938(2)–1.976(2)
C(21)–C(22)	1.488(3)		
Bond angles			
C(13)–C(14)–C(15)	142.05(19)	C(20)–O(14)–C(21)	111.76(17)
C(14)–C(15)–C(16)	141.5(2)	O(14)–C(21)–C(22)	107.82(19)
C(15)–C(16)–C(17)	141.9(2)	C(21)–C(22)–O(15)	107.6(2)
C(16)–C(17)–C(18)	140.9(2)	C(22)–O(15)–C(23)	112.92(18)
C(17)–C(18)–O(13)	109.19(18)	O(15)–C(23)–C(24)	109.23(19)
C(18)–O(13)–C(19)	111.21(17)	C(23)–C(24)–O(16)	113.51(19)
O(13)–C(19)–C(20)	109.8(2)	C(24)–O(16)–C(13)	113.91(15)
C(19)–C(20)–O(14)	109.00(19)	O(16)–C(13)–C(14)	108.79(17)

in **5a** while four are present in **5b**. Confirmation of the monomeric nature of **5a** and **5b** is revealed in their FAB mass spectra with molecular ion peaks along with fragmentation peaks corresponding to the loss of carbonyl groups from the parent ion evident.

It is uncertain why an additional dimeric species is not formed in any of the reactions of **1a** with glycols in a manner similar to that seen for the reaction of **1a** with aliphatic diols (vide supra). It would seem likely that the presence of oxygen donors within the glycolic-based nucleophile could lead to a weak Co–O interaction in an intermediate (or transition state) which would favour monomeric ring closure. Indeed, such an Co–O interaction has previously been proposed to explain the high monomer to dimer ratio observed during the reaction of **1a** with dithioethers.[9b]

3. Reaction of 1a with Diynyl-, Alkynyl- or Aryl-Linked Alkyl Diols

In order to introduce a soft donor into the macrocycle we have also targeted the reactions of alkyl diols that contain alkynyl or aryl linking units. Accordingly, the reaction of **1a** with one equivalent of the 1,3-diyne-linked alkyl diols, $HOCR_2C{\equiv}CC{\equiv}CCR_2OH$, was initially examined and found to furnish, in addition to trace quantities of **2**, monomeric $[\{Co_2(CO)_6\}_2\{$*cyclo*-μ-η^2:μ-η^2-$CH_2C_2C_2CH_2OCR_2C_2C_2CR_2O\}]$ [**6a**: R = H, **6b**: R = Me] and dimeric macrocycles $[\{Co_2(CO)_6\}_2\{$*cyclo*-μ-η^2:μ-η^2-$CH_2C_2C_2CH_2OCR_2C_2C_2CR_2O\}]_2$ [**7a** R = H, **7b** R = Me] in high combined yield (Scheme 2).

As with **3** and **4**, the similarity of the spectroscopic data for monomeric **6** with the corresponding dimeric **7** meant unequivocal identification by NMR and IR spectroscopy proved problematic (see Table 1). Nevertheless, the incorporation of the uncoordinated 1,3-diyne into the macrocycle could be confirmed by the presence of two different types of methylene protons in the ^1H NMR spectra of **6a** and **7a**, while the equivalent methyl protons in **6b** and **7b** are seen as singlets (see Table 1). In the FAB mass spectra of **6** and **7**, however, the complexes could be readily distinguished, with molecular ion peaks corresponding to monomeric and dimeric species along with fragmentation peaks that match to the loss of twelve or twenty-four successive carbonyl groups, respectively.

In order to identify unambiguously the new complexes the structure of one such complex, **7a**, was determined by a single-crystal X-ray diffraction study. Suitable crystals for the study could be grown from dichloromethane by slow diffusion of hexane at 0 °C. Selected bond lengths and angles are given in Table 5 and a view of the molecular structure is depicted in Figure 5.

The molecular structure of **7a** sits on a crystallographic centre of symmetry which lies between the alkynic bonds C(13)–C(14A) and C(13A)–C(14). The structure confirms the molecule is comprised of four $Co_2(CO)_6$ units and is bridged by a twenty-eight-membered 1,8,15,22-tetraoxacycloicosaocta-3,5,10,12,17,19,24,26-octayne ring. The geometric parameters of the pseudo-tetrahedral Co_2C_2 cores are unexceptional. As expected the *bend back* angles for the non-coordinated diyne are close to one hundred and eighty degrees [C(18)–C(19)–C(20) 177.2(3), C(21)–C(22)–C(23) 173.4°] while the coordinated ones [C(15)–C(16)–C(17) 141.2(2), C(24)–C(13)–C(14A) 138.3(2)°] fall in a range similar to previously reported acyclic cobalt-bound diyne complexes.[12–14] The two uncoordinated diyne chains adopt a parallel relative conformation with the C(22) and C(22A) separation being 3.748 Å. Examination of the coordinated C≡C–C≡C torsion angles (40.2°) reveals the Co_2C_2 units to be disposed in a pseudo *cis* configuration.

The reaction of the shorter alkynyl- or aryl-linked alkyl diols, $HOCH_2(L)CH_2OH$ (L = –C≡C–, 1,4-C_6H_4) with **1a** has also been examined. Thus treatment of **1a** with one equivalent of $HOCH_2(L)CH_2OH$ (L = –C≡C–, 1,4-C_6H_4), in the presence of $HBF_4{\cdot}OEt_2$, affords the unsymmetrical dimeric $[\{Co_2(CO)_6\}_2\{$*cyclo*-μ-η^2:μ-η^2-$CH_2C_2C_2CH_2\}_2O$-$\{OCH_2(L)CH_2O\}]$ [**8a**: L = –C≡C–, **8b**: L = 1,4-C_6H_4] and symmetrical dimeric species $[\{Co_2(CO)_6\}_2\{$*cyclo*-μ-η^2:μ-η^2-$CH_2C_2C_2CH_2OCH_2(L)CH_2O\}]_2$ [**9a**: L = –C≡C–, **9b**: L = 1,4-C_6H_4] in high combined yields (Scheme 2). Also isolated in trace quantities is the self-dimerised species **2** but there is no evidence for any monomeric species (cf. reactions of **1a** with diynyl-linked alkyl diols).

The FAB mass spectra of **8** and **9** give molecular ion peaks along with fragmentation peaks consistent with the proposed dimeric structures (see Table 1). In the IR spectra for **9** four terminal carbonyl bands are seen in a pattern similar to that observed for the other symmetrical monomeric (**3**, **5**, **6**) or dimeric (**2**, **4**, **7**) species prepared in this work. In the case of **8a** and **8b**, however, the terminal carbonyl regions are more complicated with greater than four bands evident and consistent with the dicobalt units now being in non-equivalent environments. The unsymmetrical nature of **8a** and **8b** is further supported by the ^1H NMR spectra which show three singlets for the inequivalent methylene protons, this inequivalence also being reflected in the ^{13}C NMR spectra with three singlets observed for the corresponding methylene carbon atoms.

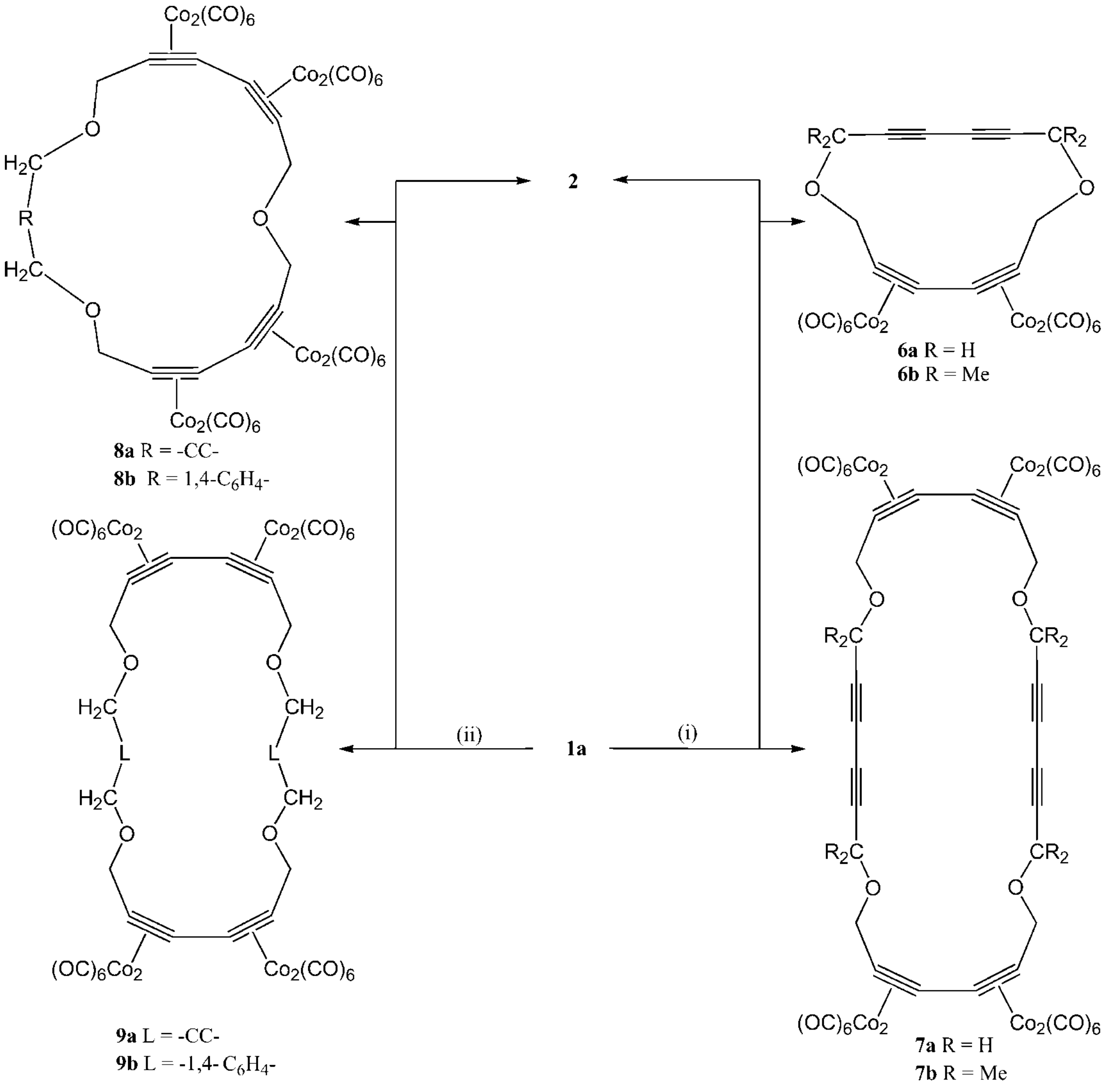

Scheme 2. Reagents and conditions; (i) $HOCR_2C_2C_2CR_2OH$, $HBF_4·OEt_2$ (cat.), –78 °C, CH_2Cl_2; (ii) $HOCH_2$-L-CH_2OH, $HBF_4·OEt_2$ (cat.), –78 °C, CH_2Cl_2.

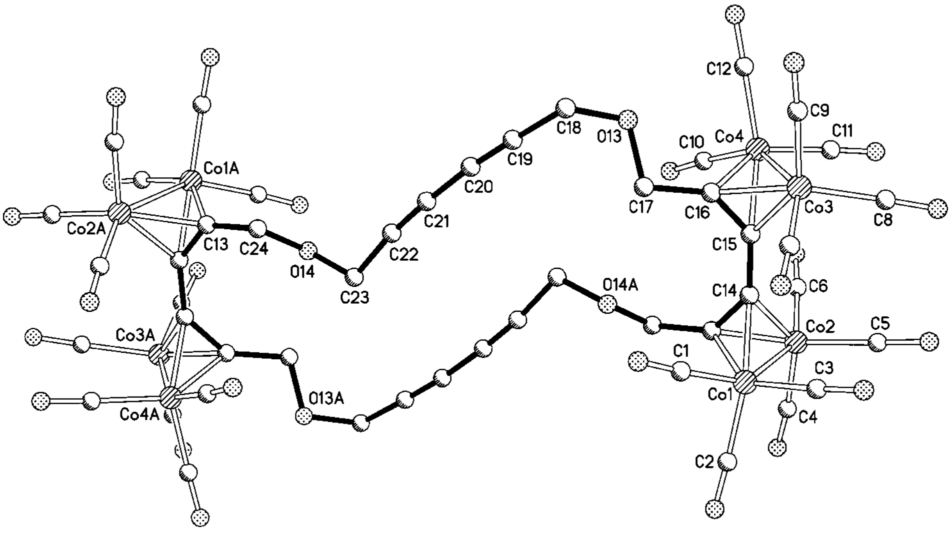

Figure 5. Molecular structure of **7a** with partial atom labeling scheme; all hydrogen atoms have been omitted for clarity.

Table 5. Selected bond lengths [Å] and angles (°) for **7a**.[a]

Bond lengths			
C(13A)–C(14)	1.353(3)	C(22)–C(23)	1.471(4)
C(14)–C(15)	1.434(3)	C(23)–O(14)	1.417(3)
C(15)–C(16)	1.358(3)	O(14)–C(24)	1.422(3)
C(16)–C(17)	1.476(3)	C(24)–C(13)	1.479(3)
C(17)–O(13)	1.426(3)	Co(1)–Co(2)	2.4701(5)
O(13)–C(18)	1.422(3)	Co(3)–Co(4)	2.4700(5)
C(18)–C(19)	1.463(4)	Co–C(carbonyl)	1.788(3)–1.831(3)
C(19)–C(20)	1.196(3)	C–O(carbonyl)	1.128(3)–1.139(3)
C(20)–C(21)	1.376(3)	Co–C(alkyne)	1.935(2)–1.968(2)
C(21)–C(22)	1.195(4)		
Bond angles			
C(13A)–C(14)–C(15)	140.0(2)	C(19)–C(20)–C(21)	175.3(3)
C(14)–C(15)–C(16)	140.3(2)	C(20)–C(21)–C(22)	176.4(3)
C(15)–C(16)–C(17)	141.2(2)	C(21)–C(22)–C(23)	173.4(3)
C(16)–C(17)–O(13)	108.49(19)	C(22)–C(23)–O(14)	114.8(2)
C(17)–O(13)–C(18)	112.56(19)	C(23)–O(14)–C(24)	112.9(2)
O(13)–C(18)–C(19)	113.9(2)	O(14)–C(24)–C(13)	107.12(19)
C(18)–C(19)–C(20)	177.2(3)	C(24)–C(13)–C(14A)	138.3(2)

[a] Atoms with suffix A are generated by symmetry (–*x* + 1/2, –*y* + 1/2, –*z*).

Confirmation of the proposed structural types was obtained from single-crystal X-ray diffraction studies that were performed on **8a**, **8b** and **9a**. Suitable crystals of each complex could be grown form dichloromethane solution by diffusion of hexane at 0 °C. Views of **8a**, **8b** and **9a** are shown in Figure 6, Figure 7 and Figure 8; selected bond lengths are angles are listed in Table 6, Table 7 and Table 8.

The molecular structure of **8a** sits on a crystallographic centre of symmetry which lies at the centre of O(13) and the mid-point of the C(21)···C(21A) and C(22)···C(22A) vectors within the phenyl ring; no such centre of symmetry is apparent in **8a**. The structures of **8a** and **8b** are similar and reveal nineteen- (**8a**) and twenty-one-membered (**8b**) macrocyclic rings with one methylene end-group in each $\{Co_2(CO)_6\}_2$(*cyclo*-μ-η^2:μ-η^2-$CH_2C_2C_2CH_2$) unit linked by an oxygen atom and the other by a $OCH_2C{\equiv}CH_2O$ (**8a**) or by a $OCH_2C_6H_4CH_2O$ (**8b**) moiety. The Co_2C_2 cores, as in related structures, adopt pseudo tetrahedral geometries with all bond lengths within the cores falling in the expected

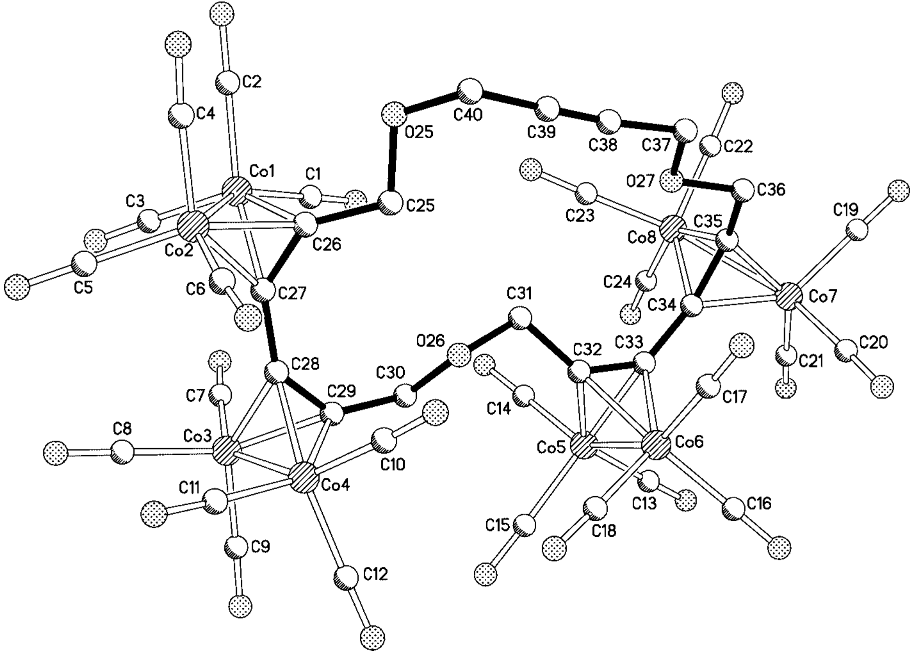

Figure 6. Molecular structure of **8a** with partial atom labeling scheme; all hydrogen atoms have been omitted for clarity.

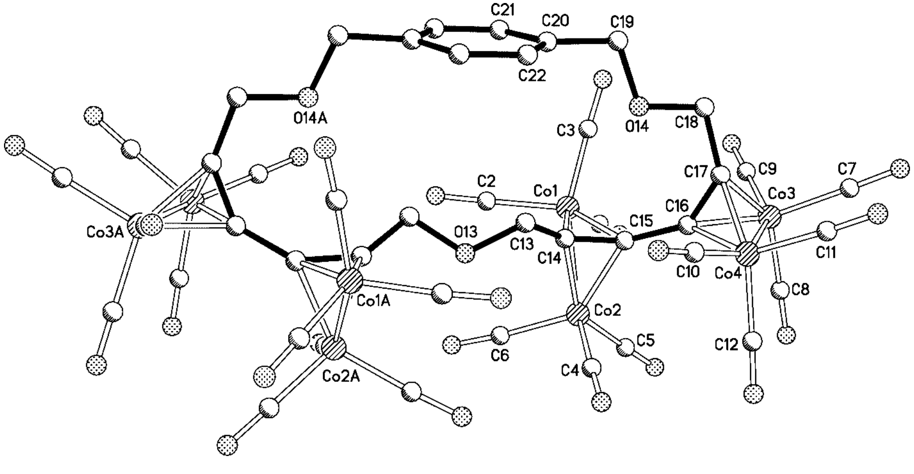

Figure 7. Molecular structure of **8b** with partial atom labeling scheme; all hydrogen atoms have been omitted for clarity.

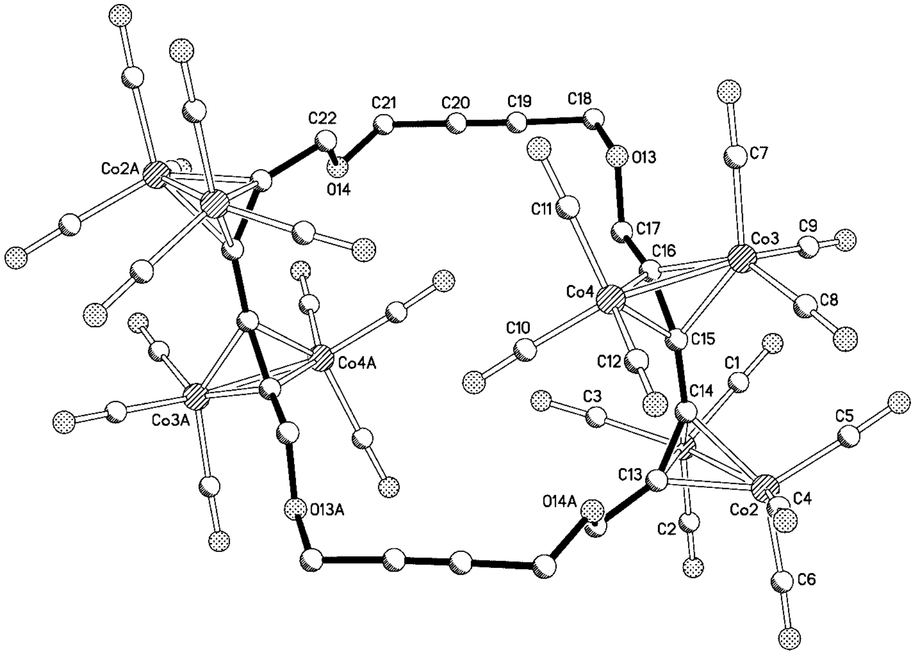

Figure 8. Molecular structure of **9a** with partial atom labeling scheme; all hydrogen atoms have been omitted for clarity.

Table 6. Selected bond lengths [Å] and angles (°) for **8a**.

Bond lengths			
C(25)–C(26)	1.475(5)	C(36)–O(27)	1.422(4)
C(25)–O(25)	1.421(4)	O(27)–C(37)	1.427(4)
C(26)–C(27)	1.349(4)	C(37)–C(38)	1.456(5)
C(27)–C(28)	1.432(4)	C(38)–C(39)	1.195(5)
C(28)–C(29)	1.351(5)	C(39)–C(40)	1.464(5)
C(29)–C(30)	1.484(5)	C(40)–O(25)	1.420(4)
C(30)–O(26)	1.415(4)	Co(1)–Co(2)	2.4699(7)
O(26)–C(31)	1.425(4)	Co(3)–Co(4)	2.4661(6)
C(31)–C(32)	1.492(5)	Co(5)–Co(6)	2.4674(7)
C(32)–C(33)	1.352(5)	Co(7)–Co(8)	2.4758(6)
C(33)–C(34)	1.430(5)	Co–C(carbonyl)	1.782(4)–1.825(5)
C(34)–C(35)	1.353(5)	C–O(carbonyl)	1.122(5)–1.140(5)
C(35)–C(36)	1.482(5)	Co–C(alkyne)	1.936(3)–1.967(3)
Bond angles			
O(25)–C(25)–C(26)	109.7(3)	C(33)–C(34)–C(35)	141.1(3)
C(25)–C(26)–C(27)	139.8(3)	C(34)–C(35)–C(36)	139.0(3)
C(26)–C(27)–C(28)	140.1(3)	C(35)–C(36)–O(27)	109.1(3)
C(27)–C(28)–C(29)	138.8(3)	C(36)–O(27)–C(37)	109.9(3)
C(28)–C(29)–C(30)	137.0(3)	O(27)–C(37)–C(38)	110.5(3)
C(29)–C(30)–O(26)	108.5(3)	C(37)–C(38)–C(39)	174.6(4)
C(30)–O(26)–C(31)	113.7(3)	C(38)–C(39)–C(40)	178.8(4)
O(26)–C(31)–C(32)	115.2(3)	C(39)–C(40)–O(25)	114.2(3)
C(31)–C(32)–C(33)	136.0(3)	C(40)–O(25)–C(25)	112.0(3)
C(32)–C(33)–C(34)	139.9(3)		

ranges for this class of compounds.[12–14] The CH$_2$–C≡C *bend back* angles reveal some differences between structures with the angle involving the O-linked methylene groups in **8a** being more strained than the OCH$_2$C≡CCH$_2$O-linked ones [C(28)–C(29)–C(30) 137.0(3), C(31)–C(32)–C(33) 136.0(3)° vs. C(34)–C(35)–C(36) 139.0(3), C(25)–C(26)–C(27) 139.8(3)°]. By contrast, in **8b** the OCH$_2$C$_6$H$_4$CH$_2$O-linked methylene groups are more strained [C(16)–C(17)–C(18) 135.1(2) vs. C(13)–C(14)–C(15) 142.0(2)°]. As with

Table 7. Selected bond lengths [Å] and angles (°) for **8b**.[a]

Bond lengths			
C(13)–O(13)	1.406(3)	C(19)–C(20)	1.501(4)
C(13A)–O(13)	1.406(3)	C(20)–C(21)	1.369(4)
C(13)–C(14)	1.484(3)	C(21)–C(22A)	1.379(4)
C(14)–C(15)	1.350(3)	C(20)–C(22)	1.367(4)
C(15)–C(16)	1.420(3)	Co(1)–Co(2)	2.4705(5)
C(16)–C(17)	1.350(3)	Co(3)–Co(4)	2.4698(5)
C(17)–C(18)	1.489(3)	Co–C(carbonyl)	1.779(4)–1.827(3)
C(18)–O(14)	1.426(3)	C–O(carbonyl)	1.125(3)–1.141(3)
O(14)–C(19)	1.430(3)	Co–C(alkyne)	1.941(2)–1.986(2)
Bond angles			
O(13)–C(13)–C(14)	109.80(19)	C(17)–C(18)–O(14)	107.7(2)
C(13)–C(14)–C(15)	142.0(2)	C(18)–O(14)–C(19)	110.97(18)
C(14)–C(15)–C(16)	140.6(2)	O(14)–C(19)–C(20)	108.9(2)
C(15)–C(16)–C(17)	138.7(2)	C(13A)–O(13)–C(13)	117.6(3)
C(16)–C(17)–C(18)	135.1(2)		

[a] Atoms with suffix A are generated by symmetry (–x, y, 1/2 – z).

Table 8. Selected bond lengths [Å] and angles (°) for **9a**.[a]

Bond lengths			
C(13)–C(22A)	1.486(3)	C(20)–C(21)	1.477(3)
C(13)–C(14)	1.349(3)	C(21)–O(14)	1.424(3)
C(14)–C(15)	1.430(3)	O(14)–C(22)	1.428(3)
C(15)–C(16)	1.356(3)	Co(1)–Co(2)	2.4786(4)
C(16)–C(17)	1.484(3)	Co(3)–Co(4)	2.4689(4)
C(17)–O(13)	1.417(3)	Co–C(carbonyl)	1.790(3)–1.830(3)
O(13)–C(18)	1.429(3)	C–O(carbonyl)	1.125(3)–1.136(3)
C(18)–C(19)	1.473(3)	Co–C(alkyne)	1.936(2)–1.976(2)
C(19)–C(20)	1.185(3)		
Bond angles			
C(13)–C(14)–C(15)	143.03(19)	C(18)–C(19)–C(20)	176.7(2)
C(14)–C(15)–C(16)	141.7(2)	C(19)–C(20)–C(21)	177.1(2)
C(15)–C(16)–C(17)	139.6(2)	C(20)–C(21)–O(14)	114.04(19)
C(16)–C(17)–O(13)	109.32(18)	C(21)–O(14)–C(22)	112.74(19)
C(17)–O(13)–C(18)	112.27(17)	O(14)–C(22)–C(13A)	107.41(19)
O(13)–C(18)–C(19)	113.82(18)	C(14)–C(13)–C(22A)	139.0(2)

[a] Atoms with suffix A are generated by symmetry (–x, –y, 1 – z).

previous structures in this work the two Co_2C_2 units within each coordinated diyne are disposed in a pseudo *cis* configuration [torsion angle C(26)–C(27)–C(28)–C(29) 39.6°, C(32)–C(33)–C(34)–C(35) 46.0° (**8a**); C(14)–C(15)–C(16)–C(17) 47.8° (**8b**)].

As with **8b**, the molecular structure of **9a** sits on a crystallographic centre of symmetry which lies in this case between bonds C(13)–C(22A) and C(13A)–C(22). The structure comprises a twenty-four-membered 1,6,13,18-tetraoxacycloicosatetra-3,8,10,15,20,22-hexayne ring containing two uncoordinated alkyne moieties and two coordinated diyne groups. Within the Co_2C_2 tetrahedral cores there are no unusual features with all bond lengths and angles falling in the expected ranges.[12–14] In contrast to previous struc-

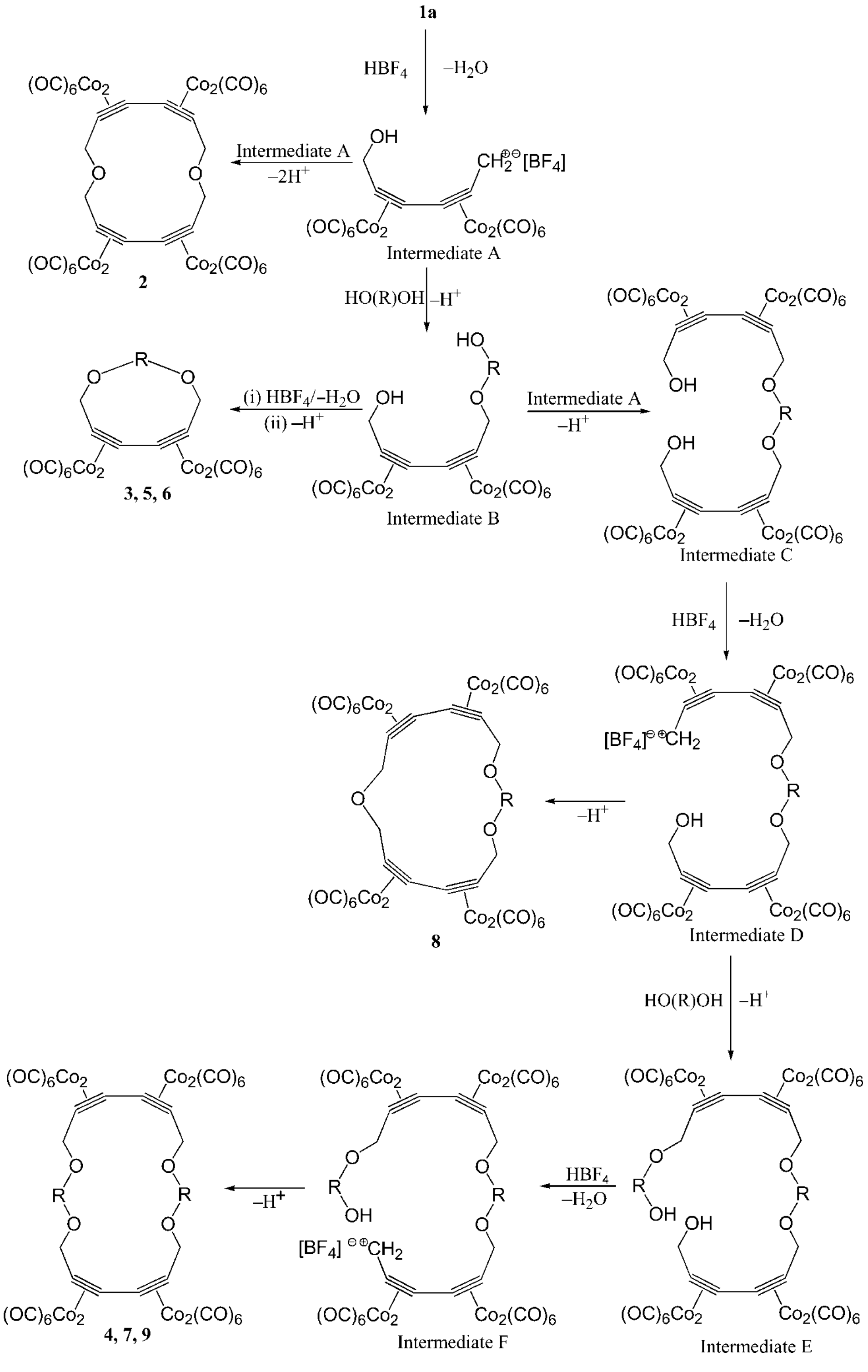

Scheme 3. Proposed pathway for the formation of **2**–**9** (R = linking unit).

tures determined in this work, the relative disposition of the two Co_2C_2 fragments on each diyne unit can be best described as pseudo *trans* [torsion angle C(13)–C(14)–C(15)–C(16) 101.7°] while the two $CH_2–C\equiv C$ *bend back* angles are comparable [139.6(2) vs. 139.0(2)°].

The formation of the unsymmetrical complexes **8** was unexpected but could be used as some indirect evidence that the Nicholas reaction chemistry outlined here occurs via sequential functionalisation at the α carbon atoms and not by a dication (e.g., $[\{Co_2(CO)_6(\mu\text{-}\eta^2\text{-}CH_2C_2\text{-})\}_2]^{2+}$).[6d,17c,19] Indeed, we have shown elsewhere that a mono-functionalised derivative can be isolated on treatment of **1a** with PhSH which can in turn be converted to a di-functionalised derivative with the same or with a different thiol-based nucleophile.[20] With these observations in mind a possible pathway for the formation of the macrocyclic complexes **2**–**9** is shown in Scheme 3.

The initial step for all products proceeds by the formation of the propargylium monocation (intermediate A) when can then can either undergo nucleophilic attack with one end of the alkyl diol, HO(R)OH to form intermediate B or undergo self dimerisation to give **2**. Intermediate B can then follow one of two pathways; for complexes **3**, **5** and **6** the generation of the cationic species derived from B results in ring closure via an intramolecular reaction. The second pathway is for intermediate B to act as nucleophile and to react with A to form intermediate C. Intermediate C can then in turn follow, via cationic intermediate D, one of two pathways to afford unsymmetrical **8** or symmetrical **4**, **7** and **9**. It would seem likely that formation of **8** would be preferred with shorter chain R groups (i.e., $CH_2C\equiv CCH_2$ or $CH_2C_6H_4CH_2$) allowing closer proximity of the intramolecular reactive partners in D. Complexes **4**, **7** and **9** are formed when D elects to undergo intermolecular nucleophilic attack with HO(R)OH to give intermediate E. Ring closure is achieved by the intramolecular reaction resulting from generation of cationic intermediate F and nucleophilic attack by the remaining hydroxy group on the chain.

4. Conclusions

Our systematic study has showed that the alkyl diols, $HOCR_2$-linker-CR_2OH (linker = alkyl, glycol, 1,3-diynyl, alkynyl, aryl; R = H, Me), can all act as effective nucleophiles on reaction with **1a** to generate crown-type macrocycles containing between and twelve and twenty eight atoms in high yields. In all cases the presence of trace quantities of the self-dimerised product **2** indicates a competitive reaction pathway that was not observed in our previous study of the reactions of thiol-based nucleophiles with **1a**.[9] The nature of the linker in the alkyl diol plays a key role in determining the monomer to dimer ratio, with monomeric **5** being uniquely favoured when **1a** is treated with glycols while with alkynyl- or aryl-linked alkyl diols solely the dimeric products **8**, **9** result; with alkyl- or 1,3-diyne-linked alkyl diols mixtures of both monomeric (**3**, **6**) and dimeric species (**4**, **7**) can be isolated. The identification of unsymmetrical dimeric species **8** when alkynyl- or aryl-linked alkyl diols nucleophiles are employed represents an unexpected observation.

Experimental Section

General Remarks: Unless otherwise stated all experiments were carried out under dry, oxygen-free nitrogen, using standard Schlenk line techniques and solvents freshly distilled from appropriate drying agent.[21] NMR spectra were recorded in $CDCl_3$ with a Bruker DRX 400 spectrometer with TMS as an external standard for ^1H and ^{13}C spectra at ambient temperature. Infrared spectra were recorded in dichloromethane solution in 0.5-mm NaCl solution cells, with a Perkin–Elmer 1710 Fourier Transform Spectrometer. FAB (Fast atom bombardment) mass spectra were recorded with a Kratos MS 890 instrument using 3-nitrobenzyl alcohol as matrix. Elemental analyses were performed by the Microanalytical Department at the University of Cambridge. Preparative TLC was carried out on 1-mm silica plates prepared at the University of Cambridge. Column chromatography was performed on Kieselgel 60 (70–230 mesh ASTM). All products are listed in order of decreasing R_f. The reagents, 1,4-butanediol, 1,5-pentanediol, 1,6-hexanediol, triethylene glycol, tetraethylene glycol, tetrafluoroboric acid (54 wt.-% in diethyl ether), 1,4-benzenedimethanol, 2-butyne-1,4-diol, 2,4-hexadiyne-1,6-diol and 2,7-dimethyl-3,5-octadiyne-2,7-diol were obtained from Aldrich Chemical Co. and used without further purification. Complex $[\{Co_2(CO)_6(\mu\text{-}\eta^2\text{-}HOCH_2C_2\text{-})\}_2]$ (**1a**) was prepared by the literature method.[17]

Reaction with $HOCH_2(CH_2)_2CH_2OH$: Six drops of $HBF_4{\cdot}OEt_2$ were added to a stirred solution of **1a** (0.50 g, 0.733 mmol) and $HOCH_2(CH_2)_2CH_2OH$ (0.07 mL, 0.764 mmol) in dichloromethane (150 mL) at –78 °C. The solution was warmed to room temperature and after 6 h an excess of sodium hydrogen carbonate was added. All volatiles were removed on the rotary evaporator, the residue taken up in hexane and the suspension filtered through a plug of magnesium sulfate. The filtrate was adsorbed onto silica, the silica pumped dry and added to the top of a chromatography column. Elution with hexane/dichloromethane (8:1) afforded orange crystalline **2** (0.10 g, 10%) and **3a** (0.15 g, 28%). Further elution of the column with hexane/dichloromethane (6:1) yielded red crystalline **4a** (0.42 g, 39%). **Complex 2:** $^{13}C\{^1H\}$ NMR ($CDCl_3$, 75 MHz): δ = 199.4 (CO), 96.6 ($C\equiv C$), 72.4 (OCH_2) ppm. **Complex 3a:** $^{13}C\{^1H\}$ NMR ($CDCl_3$, 75 MHz): δ = 199.6 (CO), 92.6, 82.6 ($C\equiv C$), 72.3, 71.6 (OCH_2), 29.7 [$OCH_2(CH_2)_2CH_2O$] ppm. **Complex 4a:** $^{13}C\{^1H\}$ NMR ($CDCl_3$, 75 MHz): δ = 191.5, 189.8 (CO), 99.2 ($C\equiv C$), 71.3, 70.9 (OCH_2), 29.7, 26.8 [$OCH_2(CH_2)_2CH_2O$] ppm.

Reaction with $HOCH_2(CH_2)_3CH_2OH$: Six drops of $HBF_4{\cdot}OEt_2$ were added to a stirred solution of **1a** (0.50 g, 0.733 mmol) and $HOCH_2(CH_2)_3CH_2OH$ (0.08 mL, 0.763 mmol) in dichloromethane (150 mL) at –78 °C. The solution was warmed to room temperature and after 6 h an excess of sodium hydrogen carbonate was added. All volatiles were removed on the rotary evaporator, the residue taken up in hexane and the suspension filtered through a plug of magnesium sulfate. The filtrate was adsorbed onto silica, the silica pumped dry and added to the top of a chromatography column. Elution with hexane/dichloromethane (8:1) afforded orange crystalline **2** (0.05 g, 5%). Further elution of the column with hexane/dichloromethane (6:1) yielded red crystalline **3b** (0.15 g, 28%) and then with hexane/dichloromethane (4:1), orange crystalline **4b** (0.32 g, 29%). **Complex 3b:** $^{13}C\{^1H\}$ NMR ($CDCl_3$, 75 MHz): δ =

196.5 (CO), 98.8 (C≡C), 71.6, 69.8 (OCH_2), 26.7, 23.5 [$OCH_2(CH_2)_3CH_2O$] ppm. **Complex 4b:** $^{13}C\{^1H\}$ NMR ($CDCl_3$, 75 MHz): δ = 199.6 (CO), 94.3 (C≡C), 72.8, 71.4 (OCH_2), 24.3, 23.5 [$OCH_2(CH_2)_3CH_2O$] ppm.

Reaction with $HOCH_2(CH_2)_4CH_2OH$: Six drops of $HBF_4·OEt_2$ were added to a stirred solution of **1a** (0.50 g, 0.733 mmol) and $HOCH_2(CH_2)_4CH_2OH$ (0.09 g, 0.762 mmol) in dichloromethane (150 mL) at –78 °C. The solution was warmed to room temperature and after 6 h an excess of sodium hydrogen carbonate was added. All volatiles were removed on the rotary evaporator, the residue taken up in hexane and the suspension filtered through a plug of magnesium sulfate. The filtrate was adsorbed onto silica, the silica pumped dry and added to the top of a chromatography column. Elution with hexane/dichloromethane (8:1) afforded orange crystalline **2** (0.10 g, 10%). Further elution of the column with hexane/dichloromethane (7:1) yielded red crystalline **3c** (0.31 g, 55%) and then with hexane/dichloromethane (4:1), orange crystalline **4c** (0.31 g, 28%). **Complex 3c:** $^{13}C\{^1H\}$ NMR ($CDCl_3$, 75 MHz): 198.9 (CO), 98.7 (C≡C), 71.3, 70.1 (OCH_2), 26.7 [$OCH_2(CH_2)_4CH_2O$]. **Complex 4c:** $^{13}C\{^1H\}$ NMR ($CDCl_3$, 75 MHz): δ = 198.9 (CO), 96.8 (C≡C), 74.2, 71.3 (OCH_2), 29.6, 25.9 [$OCH_2(CH_2)_4CH_2O$] ppm.

Reaction with $HO(CH_2CH_2O)_3H$: Four drops of $HBF_4·OEt_2$ were added to a stirred solution of **1a** (0.50 g, 0.733 mmol) and $HO(CH_2CH_2O)_3H$ (0.10 mL, 0.749 mmol) in dichloromethane (150 mL) at –78 °C. The solution was warmed to room temperature and after 12 h an excess of sodium hydrogen carbonate was added. All volatiles were removed on the rotary evaporator, the residue taken up in hexane and the suspension filtered through a plug of magnesium sulfate. The filtrate was adsorbed onto silica, the silica pumped dry and added to the top of a chromatography column. Elution with hexane/dichloromethane (8:1) afforded orange crystalline **2** (0.05 g, 5%). Further elution of the column with dichloromethane yielded deep red crystalline **5a** (0.49 g, 83%). **Complex 5a:** $^{13}C\{^1H\}$ NMR ($CDCl_3$, 75 MHz): δ = 195.6 (CO), 101.2, 82.6 (C≡C), 72.4, 71.8 (OCH_2) ppm.

Reaction with $HO(CH_2CH_2O)_4H$: Four drops of $HBF_4·OEt_2$ were added to a stirred solution of **1a** (0.50 g, 0.733 mmol) and $HO(CH_2CH_2O)_4H$ (0.13 mL, 0.753 mmol) in dichloromethane (150 mL) at –78 °C. The solution was warmed to room temperature and after 12 h an excess of sodium hydrogen carbonate was added. All volatiles were removed on the rotary evaporator, the residue taken up in hexane and the suspension filtered through a plug of magnesium sulfate. The filtrate was adsorbed onto silica, the silica pumped dry and added to the top of a chromatography column. Elution with hexane/dichloromethane (8:1) afforded orange crystalline **2** (0.10 g, 10%). Further elution of the column with dichloromethane afforded red crystalline **5b** (0.25 g, 40%). **Complex 5b:** $^{13}C\{^1H\}$ NMR ($CDCl_3$, 75 MHz): δ = 199.0 (CO), 98.8, 83.4 (C≡C), 72.0, 71.4, 71.0, 70.8 (OCH_2) ppm.

Reaction with $HOCH_2C≡CC≡CCH_2OH$: Six drops of $HBF_4·OEt_2$ were added to a stirred solution of **1a** (0.50 g, 0.733 mmol) and $HOCH_2C≡CC≡CCH_2OH$ (0.080 g, 0.736 mmol) in dichloromethane (150 mL) at room temperature. After 16 h of stirring an excess of sodium hydrogen carbonate was added. All volatiles were removed on the rotary evaporator, the residue taken up in hexane and the suspension filtered through a plug of magnesium sulfate. The filtrate was adsorbed onto silica, the silica pumped dry and added to the top of a chromatography column. Elution with hexane/dichloromethane (8:1) afforded orange crystalline **2** (0.04 g, 4%). Further elution of the column with hexane/dichloromethane (3:1) gave deep red crystalline **6a** (0.18 g, 32%) and then with hexane/dichloromethane (2:1), deep red crystalline **7a** (0.18 g, 32%). **Complex 6a:** $^{13}C\{^1H\}$ NMR ($CDCl_3$, 75 MHz): δ = 194.3 (CO), 98.4, 91.2 (C≡C), 73.2, 71.2 (OCH_2) ppm. **Complex 7a:** $^{13}C\{^1H\}$ NMR ($CDCl_3$, 75 MHz): δ = 198.7 (CO), 101.2, 82.6 (C≡C), 74.6, 71.2 (OCH_2) ppm.

Reaction with $HOC(Me)_2C≡CC≡CC(Me)_2OH$: Six drops of $HBF_4·OEt_2$ were added to a stirred solution of **1a** (0.50 g, 0.733 mmol) and $HOC(Me)_2C≡CC≡CC(Me)_2OH$ (0.081 g, 0.736 mmol) in dichloromethane (150 mL) at room temperature. After 16 h of stirring an excess of sodium hydrogen carbonate was added. All volatiles were removed on the rotary evaporator, the residue taken up in hexane and the suspension filtered through a plug of magnesium sulfate. The filtrate was adsorbed onto silica, the silica pumped dry and added to the top of a chromatography column. Elution with hexane/dichloromethane (8:1) afforded orange crystalline **2** (0.04 g, 4%). Further elution of the column with hexane/dichloromethane (4:1) gave red crystalline **6b** (0.16 g, 27%) and then with hexane/dichloromethane (2:1), orange crystalline **7b** (0.41 g, 34%). **Complex 6b:** $^{13}C\{^1H\}$ NMR ($CDCl_3$, 75 MHz): δ = 198.9 (CO), 96.4, 82.4 (C≡C), 72.6 [$OC(CH_3)_2$], 28.4 (CH_3) ppm. **Complex 7b:** $^{13}C\{^1H\}$ NMR ($CDCl_3$, 75 MHz): δ = 198.9 (CO), 98.6, 84.2 (C≡C), 72.5 [$OC(CH_3)_2$], 26.9 (CH_3) ppm.

Reaction with $HOCH_2C≡CCH_2OH$: Six drops of $HBF_4·OEt_2$ were added to a stirred solution of **1a** (0.50 g, 0.733 mmol) and $HOCH_2C≡CCH_2OH$ (0.065 g, 0.755 mmol) in dichloromethane (150 mL) at room temperature. After 16 h of stirring an excess of sodium hydrogen carbonate was added. All volatiles were removed on the rotary evaporator, the residue dissolved in hexane and the solution filtered through a plug of magnesium sulfate. The filtrate was adsorbed onto silica, the silica pumped dry and added to the top of a chromatography column. Elution with hexane/dichloromethane (8:1) afforded orange crystalline **2** (0.04 g, 4%). Further elution of the column with hexane/dichloromethane (4:1) gave deep red crystalline **8a** (0.24 g, 23%) and then with hexane/dichloromethane (3:1), deep red crystalline **9a** (0.52 g, 48%). **Complex 8a:** $^{13}C\{^1H\}$ NMR ($CDCl_3$, 75 MHz): δ = 199.9 (CO), 104.2, 94.3, 89.6 (C≡C), 74.3, 72.4, 68.2 (CH_2) ppm. **Complex 9a:** $^{13}C\{^1H\}$ NMR ($CDCl_3$, 75 MHz): δ = 194.5 (CO), 94.2, 92.6 (C≡C), 74.8, 73.2 (OCH_2) ppm.

Reaction with $HOCH_2(C_6H_4)CH_2OH$: Six drops of $HBF_4·OEt_2$ were added to a stirred solution of **1a** (0.50 g, 0.733 mmol) and $HOCH_2(C_6H_4)CH_2OH$ (0.11 g, 0.796 mmol) in dichloromethane (150 mL) at room temperature. After 16 h of stirring an excess of sodium hydrogen carbonate was added. All volatiles were removed on the rotary evaporator, the residue dissolved in hexane and the solution filtered through a plug of magnesium sulfate. The filtrate was adsorbed onto silica, the silica pumped dry and added to the top of a chromatography column. Elution with hexane/dichloromethane (8:1) afforded orange crystalline **2** (0.04 g, 4%). Further elution of the column with hexane/dichloromethane (4:1) yielded deep red crystalline **8b** (0.42 g, 40%) and then with hexane/dichloromethane (3:1), deep red crystalline **9b** (0.39 g, 34%). **Complex 8b:** $^{13}C\{^1H\}$ NMR ($CDCl_3$, 75 MHz): δ = 199.0 (CO), 137.7, 129.3 (Ph), 101.2, 97.9, 92.7 (C≡C), 73.7, 72.6, 71.7 (OCH_2) ppm. **Complex 9b:** $^{13}C\{^1H\}$ NMR ($CDCl_3$, 75 MHz): δ = 198.9 (CO), 137.6, 127.9 (Ph), 99.7, 92.7 (C≡C), 72.8, 70.6 (OCH_2) ppm.

Crystallographic Studies: Single crystal X-ray diffraction data for **2**, **3a**, **5a**, **7a**, **8a**, **8b** and **9a** were collected using a Nonius-Kappa CCD diffractometer, equipped with an Oxford Cryosystems cyrostream and employing Mo-K_α (λ = 0.71073 Å) irradiation from a sealed tube X-ray source. Cell refinement, data collection and data reduction were performed with the programs DENZO[22] and COLLECT[23] and multi-scan absorption corrections were applied to all intensity data with the program SORTAV.[24] All structures were solved and refined with the programs SHELXS97 and SHELXL97,[25] respectively. Hydrogen atoms were included in calculated positions (C–H = 0.96 Å) riding on the bonded atom with isotropic displacement parameters set to $1.5U_{eq}$(C) for methyl H atoms and $1.2U_{eq}$(C) for all other H atoms. Details of the data collection, refinement and crystal data are listed in Table 9.

CCDC-634737 (for **2**), -634738 (for **3a**), -634739 (for **5a**), -634740 (for **7a**), -63741 (for **8a**), -63743 (for **8b**) and -63742 (for **9a**) contain

Table 9. Crystallographic and data processing parameters for **2**, **3a**, **5a**, **7a**, **8a**, **8b** and **9a**.[a]

Complex	**2**	**3a**	**5a**	**7a**
Formula	$C_{36}H_8Co_8O_{26}$	$C_{22}H_{12}Co_4O_{14}$	$C_{24}H_{16}Co_4O_{16}$	$C_{48}H_{16}Co_8O_{28}$
M	1327.86	736.04	796.09	1512.05
Crystal size [mm³]	0.16 × 0.16 × 0.14	0.23 × 0.18 × 0.18	0.16 × 0.14 × 0.07	0.23 × 0.11 × 0.02
Temperature [K]	180(2)	218(2)	180(2)	180(2)
Crystal system	triclinic	monoclinic	triclinic	monoclinic
Space group	$P\bar{1}$	$P2_1/c$	$P\bar{1}$	$C2/c$
a [Å]	9.1421(2)	10.5931(2)	9.3341(3)	30.6875(9)
b [Å]	9.7436(2)	29.3338(6)	10.8973(4)	9.7804(3)
c [Å]	13.8812(3)	18.0644(2)	16.0019(5)	18.9422(3)
α [°]	81.4780(10)	90	87.727(2)	90
β [°]	75.7070(10)	102.1540(10)	77.193(2)	93.862(2)
γ [°]	68.0840(10)	90	73.997(2)	90
V [Å³]	1109.47(4)	5487.44(16)	1525.26(9)	5672.3(3)
Z	1	8	2	4
D_c [Mg·m^{-3}]	1.987	1.782	1.733	1.771
F(000)	648	2912	792	2976
μ(Mo-K_α)[mm^{-1}]	3.005	2.443	2.209	2.366
Reflections collected	29146	41586	18340	22382
Independent reflections	5084	12431	6923	6445
R_{int}	0.0572	0.0641	0.0475	0.0650
Restraints/parameters	0/316	3/710	0/397	0/379
Final *R* indices	R_1 = 0.0273	R_1 = 0.0419	R_1 = 0.0334	R_1 = 0.0364
[$I > 2\sigma(I)$]	wR_2 = 0.0639	wR_2 = 0.0917	wR_2 = 0.0609	wR_2 = 0.0848
All data	R_1 = 0.0374	R_1 = 0.0775	R_1 = 0.0581	R_1 = 0.0519
	wR_2 = 0.0674	wR_2 = 0.1043	wR_2 = 0.0683	wR_2 = 0.0923
Goodness of fit on F^2 (all data)	1.070	1.041	1.009	1.027

Complex	**8a**	**8b**	**9a**
Formula	$C_{40}H_{12}Co_8O_{27}\cdot 0.5C_6H_{14}$	$C_{44}H_{16}Co_8O_{27}$	$C_{44}H_{16}Co_8O_{28}$
M	1439.02	1448.01	1464.01
Crystal size [mm³]	0.18 × 0.16 × 0.09	0.23 × 0.14 × 0.05	0.16 × 0.14 × 0.05
Temperature [K]	220(2)	180(2)	180(2)
Crystal system	triclinic	monoclinic	triclinic
Space group	$P\bar{1}$	$C2/c$	$P\bar{1}$
a [Å]	10.6824(2)	15.6580(5)	8.9576(3)
b [Å]	15.9498(5)	10.3968(2)	10.3831(4)
c [Å]	17.1603(5)	33.3519(11)	15.6330(4)
α [°]	74.682(2)	90	104.052(2)
β [°]	80.721(2)	97.216(2)	96.197(2)
γ [°]	73.670(2)	90	107.097(2)
V [Å³]	2694.21(13)	5386.5(3)	1322.69(8)
Z	2	4	1
D_c [Mg·m^{-3}]	1.774	1.786	1.838
F(000)	1418	2848	720
μ(Mo-K_α)[mm^{-1}]	2.484	2.486	2.533
Reflections collected	28377	14546	15323
Independent reflections	12158	5984	6052
R_{int}	0.0534	0.0528	0.0541
Restraints/parameters	5/688	0/357	0/361
Final *R* indices	R_1 = 0.0437	R_1 = 0.0363	R_1 = 0.0335
[$I > 2\sigma(I)$]	wR_2 = 0.0988	wR_2 = 0.0789	wR_2 = 0.0733
All data	R_1 = 0.0731	R_1 = 0.0607	R_1 = 0.0469
	wR_2 = 0.1125	wR_2 = 0.0873	wR_2 = 0.0791
Goodness of fit on F^2 (all data)	1.011	0.978	1.041

[a] Data in common: graphite-monochromated Mo-K_α radiation, λ = 0.71073 Å; $R_1 = \Sigma||F_o| - |F_c||/\Sigma|F_o|$, $wR_2 = [\Sigma w(F_o^2 - F_c^2)^2/\Sigma w(F_o^2)^2]1/2$, $w^{-1} = [\sigma^2(F_o)^2 + (aP)^2]$, $P = [\max.(F_o^2,0) + 2(F_c^2)]/3$, where a is a constant adjusted by the program; goodness of fit = $[\Sigma(F_o^2 - F_c^2)2/(n-p)]^{1/2}$ where *n* is the number of reflections and *p* the number of parameters.

the supplementary crystallographic data for this paper. These data can be obtained free of charge from The Cambridge Crystallographic Data Centre via www.ccdc.cam.ac.uk/data_request/cif.

Acknowledgments

We acknowledge the financial support of the Engineering and Physical Sciences Research Council (EPSRC) (L. J. H.-W) and Dstl. Fort Halstead (L. J. H.-W). The help of the EPSRC mass spectrometry service, Swansea is gratefully acknowledged. Dr John E. Davies is thanked for crystal structure determinations.

---

[1] For reviews see: a) G. G. Melikyan, K. M. Nicholas, in *Modern Acetylene Chemistry* (Eds.: P. J. Stang, F. Diederich), VCH, Weinheim, **1995**, chapter 4, pp. 99–139; b) A. J. M. Caffyn, K. M. Nicholas, in *Comprehensive Organometallic Chemistry II* (Eds.: E. W. Abel, F. G. A. Stone, G. Wilkinson), Pergamon, Oxford, **1995**, vol. 12, chapter 7, pp. 685–702; c) K. M. Nicholas, *Acc. Chem. Res.* **1987**, *20*, 207–214; d) B. J. Teobald, *Tetrahedron* **2002**, *58*, 4133–4170.

[2] a) M. Isobe, R. Nishizawa, S. Hosokawa, T. Nishikawa, *Chem. Commun.* **1998**, 2665–2676; b) N. Ortega, T. Martin, V. S. Martin, *Org. Lett.* **2006**, *8*, 871–873 and refs therein; c) C. Mukai, S. Yamaguchi, Y. Sugimoto, N. Miyakoshi, E. Kasamatsu, M. Hanaoka, *J. Org. Chem.* **2000**, *65*, 6761–6765.

[3] a) A. Gelling, G. F. Mohmand, J. C. Jeffery, M. J. Went, *J. Chem. Soc., Dalton Trans.* **1993**, 1857–1862; b) A. Gelling, J. C. Jeffery, D. C. Povey, M. J. Went, *J. Chem. Soc., Chem. Commun.* **1991**, 349–351; c) F. Demirhan, A. Gelling, S. Irisli, J. C. Jeffery, S. N. Salek, O. S. Senturk, M. J. Went, *J. Chem. Soc., Dalton Trans.* **1993**, 2765–2773; d) F. Demirhan, S. Irisli, S. N. Salek, O. S. Senturk, M. J. Went, J. C. Jeffery, *J. Organomet. Chem.* **1993**, *453*, C30–C31; e) S. C. Bennett, J. C. Jeffery, M. J. Went, *J. Chem. Soc., Dalton Trans.* **1994**, 3171–3176.

[4] E. Alvaro, M. C. de la Torre, M. A. Sierra, *Chem. Commun.* **2006**, 985–987.

[5] G. G. Melikyan, M. A. Khan, K. M. Nicholas, *Organometallics* **1995**, *14*, 2170–2172.

[6] a) R. Guo, J. R. Green, *Chem. Commun.* **1999**, 2503–2504; b) R. Gibe, J. R. Green, G. Davidson, *Org. Lett.* **2003**, *5*, 1003–1005; c) R. Gibe, J. R. Green, *Chem. Commun.* **2002**, 1550–1551; d) R. Guo, J. R. Green, *Synlett* **2000**, 746–748.

[7] See for example: a) R. M. Izatt, K. Pawlak, J. S. Bradshaw, R. L. Breuning, *Chem. Rev.* **1991**, *91*, 1721–1785; b) L. F. Lindoy, *Pure Appl. Chem.* **1997**, *69*, 2179–2186; c) F. Neve, M. Ghedini, M. Francescangeil, *Liq. Cryst.* **1996**, *21*, 625–630; d) A. J. Blake, A. Taylor, M. Schröder, *J. Chem. Soc., Chem. Commun.* **1993**, 1097–1098.

[8] P. I. Dosa, C. Erben, V. S. Iyer, K. P. C. Vollhardt, I. M. Wasser, *J. Am. Chem. Soc.* **1999**, *121*, 10430–10431.

[9] a) J. E. Davies, L. J. Hope-Weeks, M. J. Mays, P. R. Raithby, *Chem. Commun.* **2000**, 1411–1412; b) L. J. Hope-Weeks, M. J. Mays, A. D. Woods, *J. Chem. Soc., Dalton Trans.* **2002**, 1812–1819.

[10] R. C. J. Atkinson, L. J. Hope-Weeks, M. J. Mays, G. A. Solan, *J. Organomet. Chem.* **2007**, *692*, 2076–2085.

[11] V. B. Golovko, L. J. Hope-Weeks, M. J. Mays, M. McPartlin, A. M. Sloan, A. D. Woods, *New J. Chem.* **2004**, *28*, 527–534.

[12] a) X.-N. Chen, J. Zhang, S.-L. Wu, Y.-Q. Yin, W.-L. Wang, J. Sun, *J. Chem. Soc., Dalton Trans.* **1999**, 1987–1992; b) C. E. Housecroft, B. F. G. Johnson, M. S. Khan, J. Lewis, P. R. Raithby, M. E. Robson, D. A. Wilkinson, *J. Chem. Soc., Dalton Trans.* **1992**, 3171–3178.

[13] a) V. B. Golovko, M. J. Mays, A. D. Woods, *New J. Chem.* **2002**, *26*, 1706–1708; b) B. F. G. Johnson, J. Lewis, P. R. Raithby, D. A. Wilkinson, *J. Organomet. Chem.* **1991**, *408*, C9–C12; c) E. Champeil, S. M. Draper, *J. Chem. Soc., Dalton Trans.* **2001**, 1440–1447; d) M. B. Nielsen, N. F. Utesch, N. N. P. Moonen, C. Boudon, J.-P. Gisselbrecht, S. Concilio, S. P. Piotto, P. Seiler, P. Gunter, M. Gross, F. Diederich, *Chem. Eur. J.* **2002**, *8*, 3601–3613; e) M. I. Bruce, B. W. Skelton, M. E. Smith, A. H. White, *Aust. J. Chem.* **1999**, *52*, 431–435; f) Q.-L. Suo, L.-M. Han, Y.-B. Wang, J.-H. Ye, N. Zhu, X.-B. Leng, J. Sun, *J. Coord. Chem.* **2004**, *57*, 1591–1601.

[14] B. J. Rausch, R. Gleiter, F. Rominger, *J. Chem. Soc., Dalton Trans.* **2002**, 2219–2226.

[15] For use of the CH_2–C≡C *bend-back* angles as an indicator of strain present in alkyne-/diyne-containing macrocycles see refs. 3b, 9, 10.

[16] Calculated from a CCDC search, F. H. Allen, O. Kennard, *Chem. Design Automation News* **1993**, *8*, 31.

[17] a) G. F. Mohmand, K. Thiele, M. J. Went, *J. Organomet. Chem.* **1994**, *471*, 241–248; b) A. Osella, L. Milone, C. Nervi, M. Ravera, *Eur. J. Inorg. Chem.* **1998**, 1473–1477; c) Amouri, C. Da Silva, B. Malezieux, R. Andres, J. Vaissermann, M. Gruselle, *Inorg. Chem.* **2000**, *39*, 5053–5058.

[18] P. Groth, *Acta Chem. Scand. Ser. A* **1978**, *32*, 279–280.

[19] a) S. C. Bennet, M. A. Philipis, M. J. Went, *J. Chem. Soc., Chem. Commun.* **1994**, 225–239; b) G. G. Melikyan, A. Deravakian, S. Myer, S. Yadegar, K. I. Hardcastle, J. Ciurash, P. J. Toole, *J. Organomet. Chem.* **1999**, *578*, 68–75.

[20] L. J. Hope-Weeks, M. J. Mays, C. Paredes, G. A. Solan, *Can. J. Chem.* **2007**, submitted.

[21] W. L. F. Armarego, D. D. Perrin, “*Purification of Laboratory Chemicals*”, Butterworth Heinemann, 4th ed., **1996**.

[22] Z. Otwinowski, W. Minor, *Methods Enzymol.* **1997**, *276*, 307–326.

[23] R. Hooft, *COLLECT*, Nonius BV, Delft, The Netherlands, **1998**.

[24] R. H. Blessing, *Acta Crystallogr., Sect. A* **1995**, *51*, 33–38.

[25] G. M. Sheldrick, *SHELXS97 and SHELXL97*, University of Göttingen, Germany, **1997**.

Received: January 28, 2007
Published Online: May 10, 2007